ADVANCED FUNCTIONAL MATERIALS
www.afm-journal.de

www.MaterialsViews.com

Highly Conductive Microfiber of Graphene Oxide Templated Carbonization of Nanofibrillated Cellulose

*Yuanyuan Li, Hongli Zhu, Fei Shen, Jiayu Wan, Xiaogang Han, Jiaqi Dai, Hongqi Dai, and Liangbing Hu**

Microfibers with conductivity of 649 ± 60 S/cm are introduced through a carbonization of well-aligned graphene oxide (GO) – nanofibrillated cellulose (NFC) hybrid fibers. GO acts as a template for NFC carbonization, which changes the morphology of carbonized NFC from microspheres to sheets while improving the carbonization of NFC. Meanwhile, the carbonized NFC repairs the defects of reduced GO (rGO) and links rGO sheets together. The GO templated carbonization of NFC as well as the alignment of the building blocks along the fiber direction leads to excellent conductivity. Conductive microfibers are evaluated as lithium ion battery anodes, which can be applied in wearable electronics. This approach to make conductive microfibers and the low cost raw materials used in this work may be applied to other carbon based conductive structures.

1. Introduction

Flexible and wearable electronics are becoming popular due to their portability and integrability.[1] Conductive fibers can be easily woven into textiles or integrated into other structures to form wearable nanogenerators,[2] supercapacitors,[3] batteries,[4] actuators,[5] and flexible solar cells.[6] Carbon nanotubes (CNTs) have been widely used in the fabrication of high performance conductive microfibers due to their extraordinary mechanical properties and electrical conductivity; however, the cost for fabricating high quality CNTs, especially single wall carbon nanotubes, can not be neglected.[7,8]

Cellulose is one of the most abundant renewable natural polymers. It has been demonstrated as a precursor to form carbonaceous materials, which is important in energy storage, carbon fiber fabrication, water purification, ion exchange, catalysis, green electronics, and life science.[9–11] High temperature carbonization in a given atmosphere and hydrothermal carbonization are two promising techniques to accomplish the conversion from cellulose to carbonaceous materials.[12,13] Despite the fact that carbon structures form after releasing non-carbon atoms during the carbonization process, the conductivity of carbonized cellulose material is still low.[14–16] One strategy to enhance the conductivity of carbonized materials is to improve the graphitic structure of the carbonized product by increasing the carbonization temperature, which is also called graphitization. This stage enhances the order of the graphene stacks.[13] Graphitization is usually carried out at temperatures higher than 900 °C. A conductivity of 100 S/cm is obtained when the carbonization temperature is higher than 2000 °C;[17] however, such high temperatures require expensive equipment and are energy consuming.

Chemically exfoliated graphene oxide (GO) is a two-dimensional (2D) material, with rich hydroxyl, carboxyl, and epoxide functional groups on the basal planes and the planar edges.[18] It has been reported that GO may act as a template to assemble materials, to form novel structures or even to alternate molecular configurations.[19–22] Carbonization of GO filled poly(acrylonitrile) (PAN) nanofibers demonstrates that GO can function as a template to improve the graphitic order and orientation in PAN carbon nanofibers.[23] Studies also show that adding a very small amount of GO to glucose results in more conductive carbonized materials with higher degree of carbonization.[24] Thick layers of reduced GO (rGO) sheets are obtained, which is different from the spherical particles obtained from carbonization of pure cellulose. Such phenomena suggest that GO can be used as a template for cellulose carbonization. In addition, GO is a low cost building block to make highly conductive microfibers. rGO microfibers with a conductivity of 570 S/cm and 416 S/cm have been reported to be formed by chemical reduction and thermal reduction, respectively.[25,26] For the first time, we reported highly conductive microfibers based on GO and nanofibrillated cellulose (NFC) with GO serving as a template for cellulose carbonization, and carbonized NFC repairing the defects of carbonized/reduced GO (rGO) and linking rGO sheets together. **Figure 1**a–b show the morphology change of NFC from fibers to spherical particles after carbonization. In the carbonized GO+NFC (c(GO+NFC)) microfibers, only

Y. Y. Li,[+] H. L. Zhu,[+] F. Shen, J. Y. Wan, X. G. Han, J. Q. Dai, L. B. Hu
Department of Materials Science and Engineering
University of Maryland College Park
MD 20742, USA
E-mail: binghu@umd.edu
Y. Y. Li, Prof. H. Q. Dai
College of Light Industry Science and Engineering
Nanjing Forestry University
Nanjing, Jiangsu 210037, P. R. China
[+]These authors contributed equally to this work

DOI: 10.1002/adfm.201402129

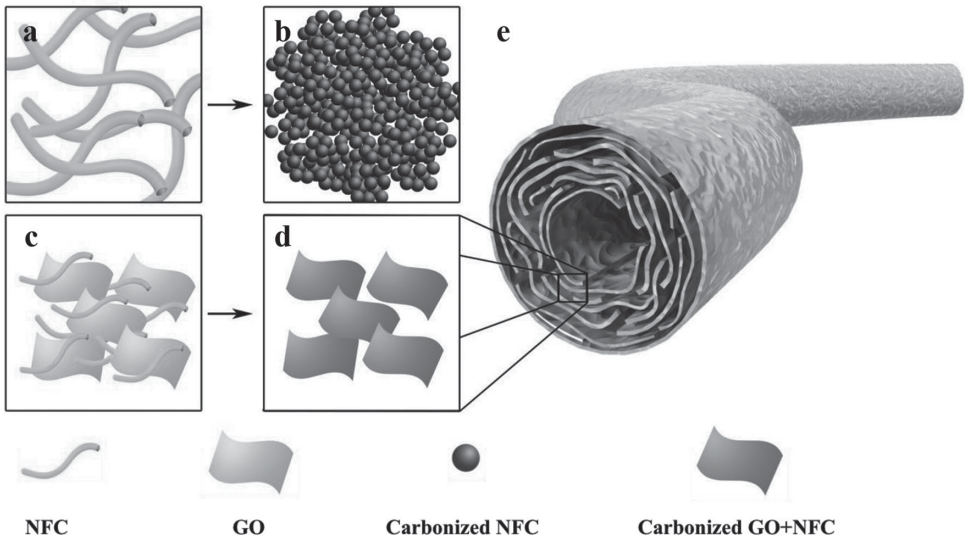

Figure 1. a–b) Schematic to show the morphology of NFC changed from fibers (before carbonization) to sphere particles after carbonization. In the c(GO+NFC) microfiber, only sheets formed after carbonization, no particles observed as shown in (c–d). e) is the structure of a c(GO+NFC) microfiber. The c(GO+NFC) microfiber shows a hollow structure with building blocks well aligned along the fiber direction.

sheets formed via the GO templates (Figure 1c–d). Figure 1e exhibits the structure of a carbonized GO+NFC microfiber. The c(GO+NFC) microfiber shows a hollow structure with building blocks well aligned along the fiber direction.

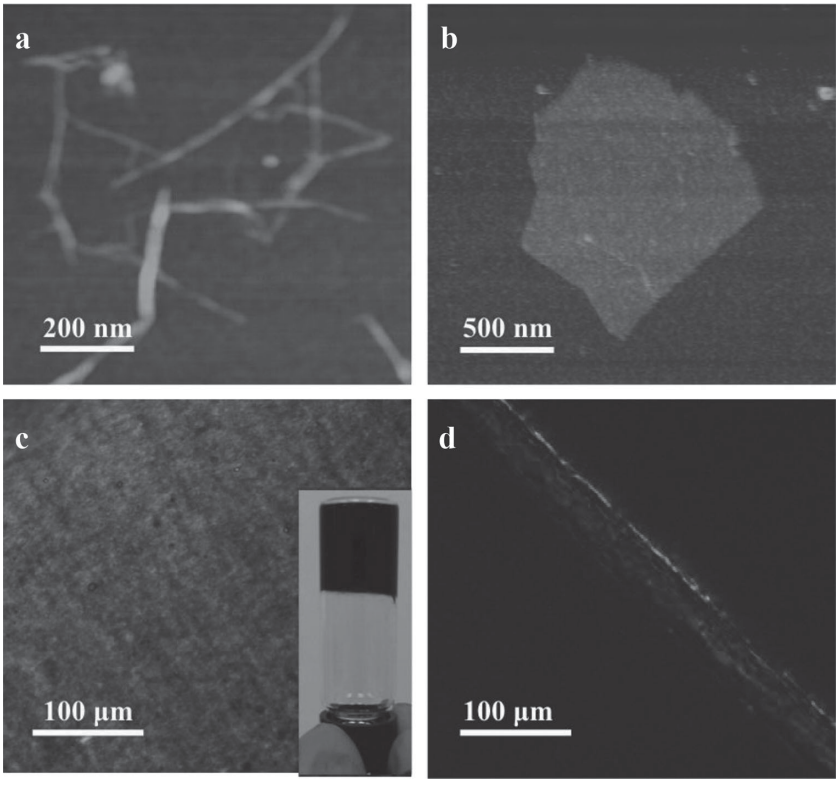

Figure 2. a) an AFM image of NFC, b) an AFM image of GO flake, c) POM image of GO water solution with 50 wt% of NFC, inset is the optical image of GO+NFC gel, d) POM image of GO+NFC fiber.

2. Results and Discussion

Cellulose has been studied to make conductive carbon fibers and carbon spheres by carbonization due to its low cost and high purity.[27] The cellulose undergoes thermal cleavage of the glycosidic linkage, scission of the ether bonds and depolymerization to monosaccharide derivatives, and finally forms carbon structures after releasing gases containing non-carbon atoms (O, H).[14] We use NFC as a carbon source to make conductive fibers. The NFC used in this work was prepared by 2,2,6,6-tetramethylpiperidine-1-oxyl (TEMPO) oxidation of wood cellulose and then disintegrated with a microfluidizer. The obtained NFC is shown in **Figure 2**a. GO was prepared by Hummer's method with an average lateral size of 1.2 μm.[28] Figure 2b shows a typical image of a GO sheet. Improving the alignment and packing density of building blocks can largely increase the fiber conductivity; for example, the conductivity of CNT microfiber with strong alignment and a high density can reach 2.9×10^4 S/cm.[8] We demonstrate well-aligned GO+NFC microfibers, which are the precursor fiber for highly conductive microfibers fabrication. Alignment of precursor fibers was achieved by using a liquid crystal spinning solution and drying the fiber under tension, which has been proved to be vital to create super-aligned fibers.[29] A GO and NFC mixed solution forms liquid crystals easily as shown in Figure 2c. Concentrating the mixed solution will result in a homogenous

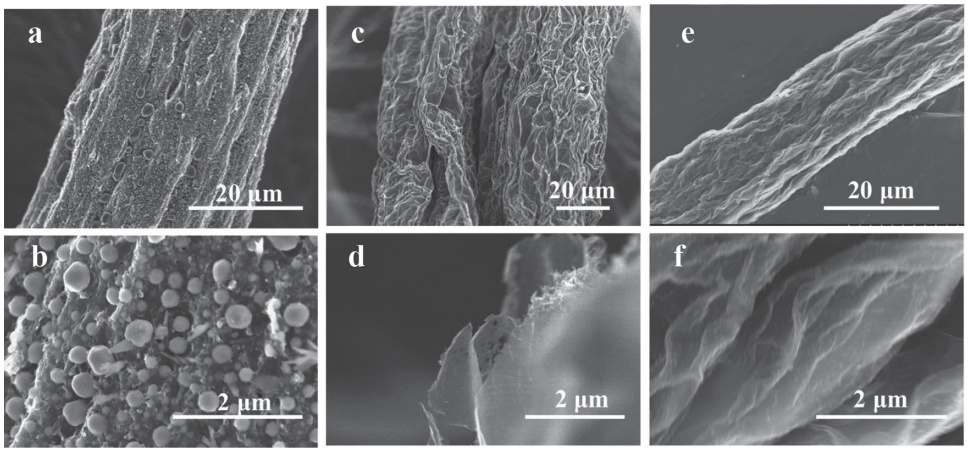

Figure 3. a,b) show the SEM images of carbonized NFC microfiber consisting of microspheres with a diameter less than 1 μm. c,d) show the SEM images of rGO microfiber consisting of rGO sheets. e,f) show the SEM images of c(GO+NFC) microfiber consisting of sheets without microspheres.

gel (the inset of Figure 2c). The well-aligned precursor fibers were fabricated by extruding the gel solution through a syringe directly into ethanol and then drying in air, which was a widely used method (wet-spinning method) in commercial fiber fabrication such as viscose rayon. A pre-stressing force by hand was applied at the ends of the fibers during drying to further improve the alignment. Polarized optical microscopy (POM) images of GO+NFC fibers were taken to prove the alignment of fibers (Figure 2d). When the well-aligned fibers were set parallel to the polarizer, only a dark image was obtained since the polarized light passed through the fibers was negated at the orthogonal analyzer. The image started to become brighter and reached its brightest mode when the fibers were rotated to 45° with respect to the polarizer. The fiber diameters varied from 10 μm to about 100 μm by changing syringe needles with different diameters. Pure NFC and GO microfibers were also made as control samples.

The average conductivity for the carbonized NFC microfibers is 33 S/cm, which is similar to that of a carbon fiber.[14] A typical current–voltage (*I–V*) curve of carbonized NFC microfibers is shown in Figure S1a. The carbonized NFC microfibers consist of many microspheres with a diameter less than 1 μm (**Figure 3**a–b), which is a typical morphology of hydrothermal carbonized cellulose.[15,30] The rGO microfiber possessed a porous structure, and rGO was still in the sheet form (Figure 3c–d). The rGO microfibers have an average conductivity of 137 S/cm, which is higher than that of carbonized NFC microfibers. This may attribute to the high conductivity of rGO. Another possible reason is that the carbonized NFC microfibers are composed of spherical particles, which possess less percolation between building blocks compared to rGO microfibers with building blocks of rGO sheets. Figure S1b shows the typical *I–V* curve of rGO microfibers. The GO itself is insulating due to the grafting of oxygen functional groups in the preparation of GO from a graphite process, which leads to the disruption of sp^2 bonding networks.[31] Thermal reduction can remove the functional groups and restore the conductivity; however, vacancies and topological defects will inevitably form, making the conductivity of the rGO lower than graphene.[32] After adding NFC in the GO fiber, c(GO+NFC) fibers possess the same porous structure as rGO microfibers. No aggregates of microspheres can be found in the fiber (Figure 3e–f), which is similar to the hydrothermal carbonized cellulose in the presence of 1 wt% GO.[24] This is because GO acts as a template for the cellulose carbonization, changing the morphology of carbonized NFC from microspheres to "coating layer" on the rGO sheets. The coating layer of carbonized NFC can repair the vacancies and topological defects formed during GO thermal reduction. In addition, the carbonized NFC coating also serves as a conductive binder to bridge the individual rGO components, thus further improves the conductivity.

The conductivity of c(GO+NFC) microfibers is 649 ± 60 S/cm, which is the highest value among reported rGO/graphene microfibers or reduced GO composite microfibers. We report a higher conductivity than thermally rGO microfibers annealed at 2000 °C, despite our fibers being carbonized at 1000 °C.[26] This value is even 79 S/cm higher than that of chemically reduced GO microfibers.[25] Conductivities of rGO/graphene microfibers or rGO composite microfibers are summarized in **Figure 4**a. The conductivity obtained in this work is even compatible to CNT based composite microfibers and part of pure CNT microfibers spinning from CNT arrays.[7,33] Figure 4b is a typical *I–V* curve of c(GO+NFC) microfibers at room temperature. Despite the high conductivity of c(GO+NFC) microfibers, Raman spectra show a lot of defects in the c(GO+NFC) microfiber (Figure 4c). In carbon materials, the band at about 1580 cm^{-1} is originated in the crystalline carbon in the graphite, which is assigned to the graphite-band (G-band). The band at about 1350 cm^{-1} is assigned to the disorder-band (D-band) originated from the defects in the lattice and the carbon with dangling bonds.[34] A high I_D/I_G ratio typically means low conductivity for carbon materials.[11,14] It is interesting that the I_D/I_G ratio of c(GO+NFC) microfiber is 1.68, which is higher than that of a pure rGO microfiber (1.45). The lowest I_D/I_G ratio was obtained from carbonized NFC microfiber, with a value of 1.17. The counterintuitive relationship between I_D/I_G ratio and conductivity of rGO microfibers and c(GO+NFC) microfibers is similar to that of the chemical vapor deposition repaired GO.[35] V. Lopez reports that this contradiction maybe due to the amorphous "coating layer" on the rGO sheet and the creation of

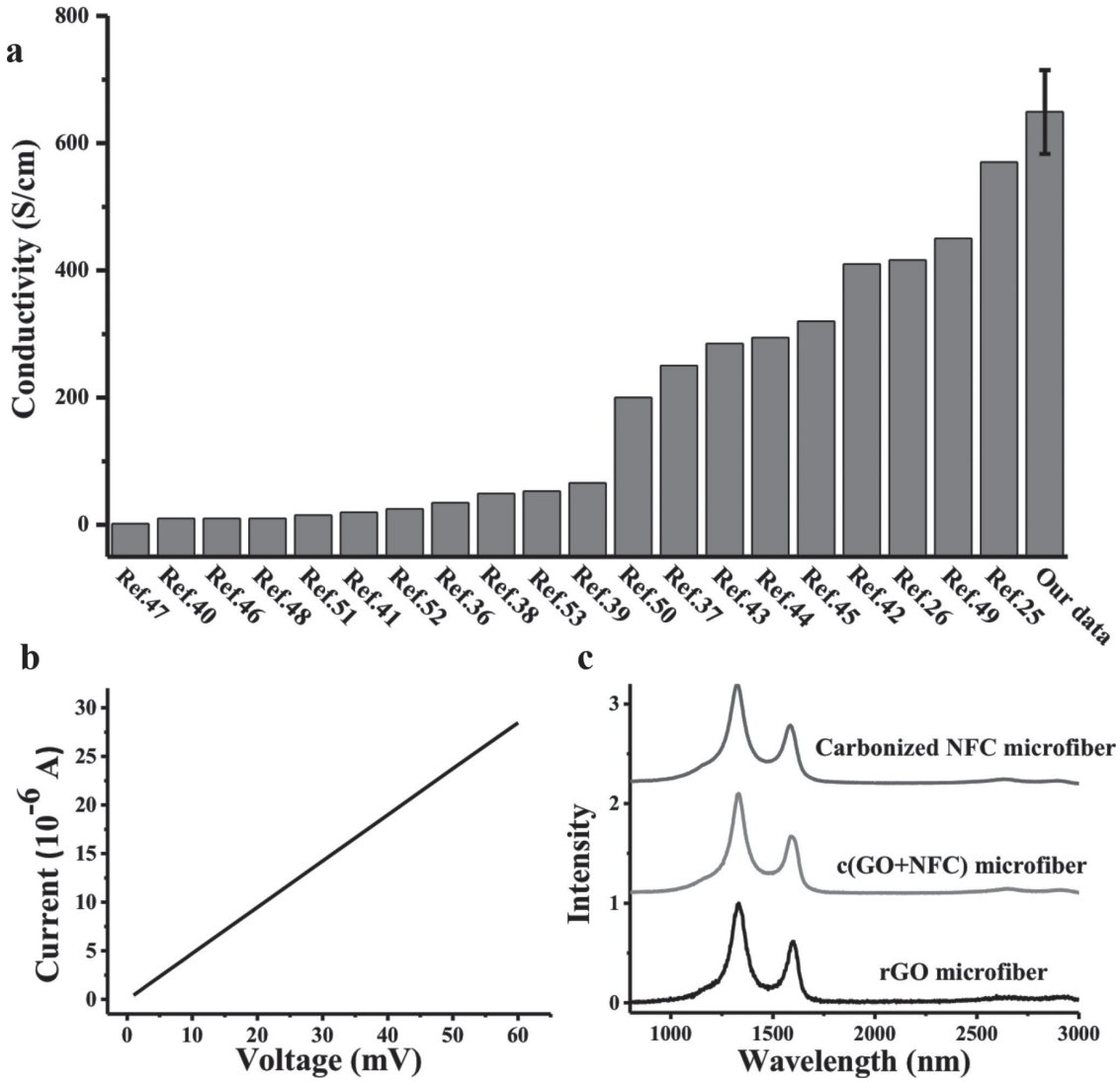

Figure 4. a) is the conductivities of rGO/graphene microfibers and reduced GO composite microfibers from literature and this work,[25,26,36–53] b) is a typical *I–V* curve of c(GO+NFC) microfiber with fiber length of 35 mm and average diameter of 18 μm, c) shows the Raman spectrum of carbonized NFC microfiber, c(GO+NFC) microfiber and rGO microfiber.

small patches of graphene within holes of the rGO sheet.[35] In c(GO+NFC) microfibers, an amorphous carbonized NFC "coating layer" may form small patches within the vacancies on rGO sheets, leading to a high I_D/I_G ratio.

A strategy for enhancing the conductivity of carbonized fibers is to improve the ordering of the graphitic structures inside each fiber. Besides a higher carbonization temperature, increasing the alignment of building blocks inside the precursor fibers is an important way. The precursor fibers we made for the fabrication of c(GO+NFC) microfibers were highly aligned as shown in **Figure 5**a–c. NFC acts as a glue for the GO sheets, giving the fibers a smooth surface and highly compacted structure (Figure S1c–d). The cross-section of the fibers shows that GO sheets are uniformly aligned toward the fiber axis direction (Figure 5c). After carbonization, the c(GO+NFC) microfibers remain highly aligned (Figure 5d–f). The alignment also improves the percolation between building blocks, which facilitates the electron transportation between building blocks and leads to high conductivity.[44] From Figure 5e, it is clear that the c(GO+NFC) microfiber is porous. The porous structure is mainly due to the volume and morphology change of NFC and GO sheets during carbonization process.[54,55] It is notable that the hollow microfibers formed after carbonization, as shown in Figure 5e, which may be due to the shrinking and restacking of building blocks during carbonization. This hollow porous structure of the microfibers offers potential applications in the field that need both high conductivity and high surface area.

Another possible reason for the high conductivity is that GO acts as a template for cellulose carbonization, increasing the carbonization of NFC and changing the morphology of carbonized NFC from microspheres to "coating layer" on the rGO sheets.[17,24] Figure S2 shows the thick layered rGO with carbonized NFC on it. The coating of the conductive layer will reduce the influence of the defective part of rGO and bind rGO

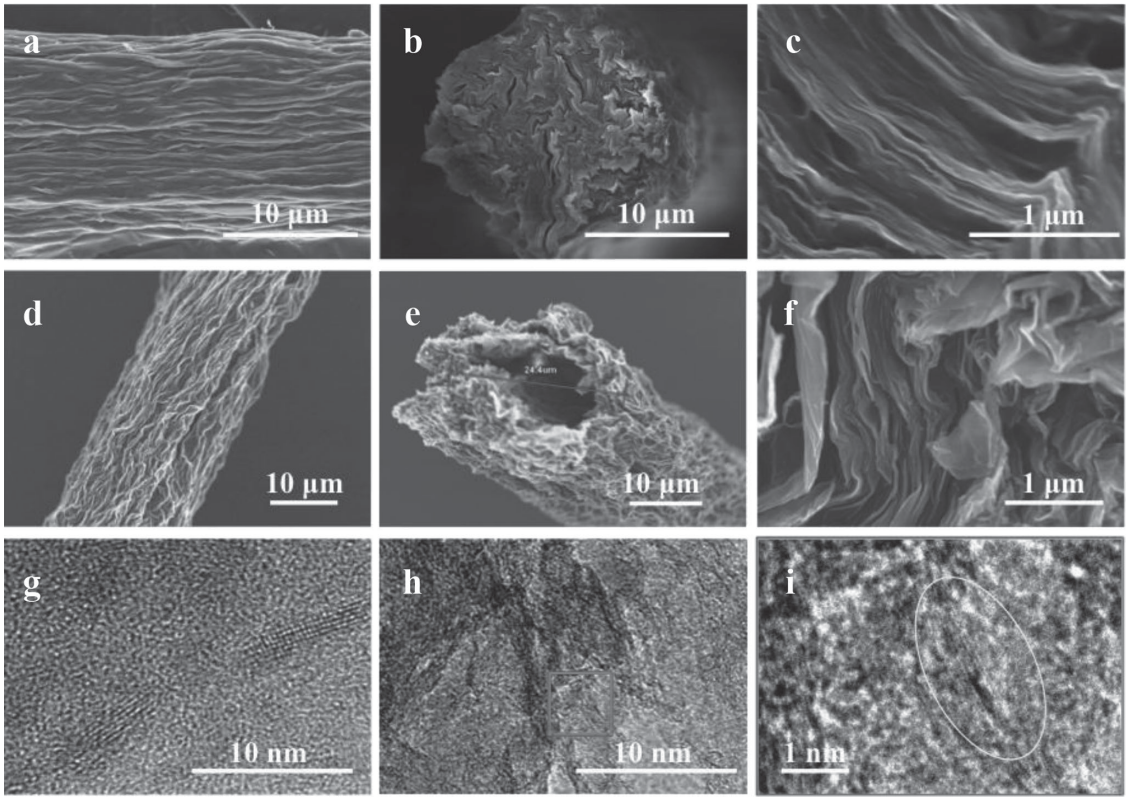

Figure 5. a–c) SEM images of as-spun GO+NFC fiber surface before carbonization (a), low resolution of cross section (b), high resolution of cross section (c). d–f) SEM images of GO+NFC fiber after carbonization, (d) is surface, (e) is low resolution of cross section, (f) is high resolution of cross section. g) TEM image of carbonized NFC microfiber. h–i) TEM images of c(GO+NFC) microfiber.

together, which enhances the conductivity of the c(GO+NFC) microfibers. In addition, the GO templates can improve the oriented graphitic crystallites of the carbonized product, which further improves the conductivity.[23] Figure 5g is a high resolution TEM image of carbonized NFC microfiber showing that the carbonized product has a large amount of amorphous carbon with a small region of graphitic lattices. More images are shown in Figure S3. Similar results were reported for cellulose nanocrystals carbonization.[56] In the c(GO+NFC) microfibers, the carbonized product shows more graphitic lattices. Figure 5h-i show representative graphitic structure in the c(GO+NFC) fiber. More details are shown in Figure S4. TEM images of rGO microfibers were also taken. Figure S5 shows that a large amount of lattice defects are homogeneously distributed throughout the rGO sheets with only a small region of graphitic structure. The carbon structure of NFC on GO template in this work is similar to that of electrospinning cellulose nanofibers carbonized at 1500 °C, which is primarily crystalline.[57] GO templated carbonization of NFC into well-aligned c(GO+NFC) fibers to repair the defects of rGO and maintain conductive bridges between the individual rGO components was used to obtain a highly conductive fiber. This preparation method can be applied to other carbon materials to make highly conductive fibers or various conductive structure materials, such as a conductive film or an aerogel.

The highly conductive fiber has potential applications in high performance wearable electronics. The electrochemical performance of c(GO+NFC) microfiber was evaluated with the c(GO+NFC) microfiber as the negative electrode and lithium metal as the counter electrode over a voltage range of 0.05–2.0 V. The charge (lithiation)/discharge (delithiation) profile of the second cycle at 25 mA/g is shown in **Figure 6**a. The second cycle has an initial discharge capacity at 317.3 mAh/g with a Columbic efficiency of 62.2%. The Columbic efficiency of the first cycles is low (28.7%) due to the formation of solid electrolyte interface (SEI) and the irreversible side reaction between lithium and functional groups (like -O-, -OH, C = O) on rGO sheets. Future research to improve the first cycle Columbic efficiency is in progress in our lab. The discharge capacity remains 312 mAh/g at the 63th cycle with tiny decay compared to the second cycle discharge capacity, Figure 6(b). The good electrochemical performance is due to the fact that the c(GO+NFC) microfibers possess high electrical conductivity.

3. Conclusion

In conclusion, microfibers with a high conductivity of 649 ± 60 S/cm were made based on earth abundant and low cost GO and NFC. The fibers were well aligned with a carbonized NFC coating on the rGO sheet. GO acts as a template for NFC carbonization, changing the morphology of the carbonized NFC from microspheres to sheets while improving the carbonization of NFC. The carbonized NFC can effectively

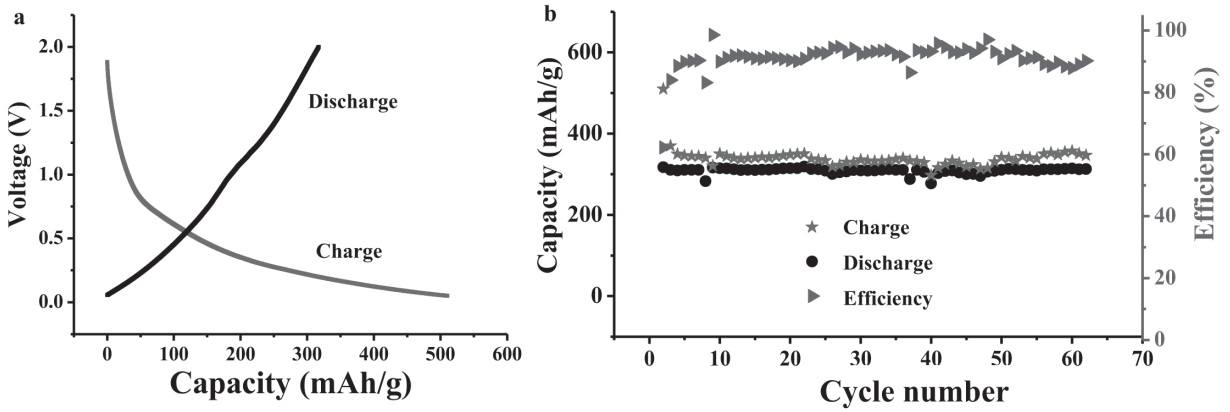

Figure 6. a) Charge (lithiation) and discharge (delithiation) voltage profile of fiber battery for the second cycle. b) Charge/discharge capacity and corresponding Coulombic efficiency cycled at a constant current density of 25 mA/g. The data are from the second cycle to the 63rd cycle.

repair the defects of rGO and bridge the rGO together. Both the high alignment of the building blocks and the GO templated carbonization of NFC lead to highly conductive fibers. Fibers were demonstrated as lithium ion battery anodes, with a stable discharge capacity of 312 mAh/g. The approach to make conductive fibers in this work could be applied to other carbon based conductive structures. The obtained highly conductive fibers thus have a great potential in a range of applications, such as wearable electronics and low-cost energy storage.

4. Experimental Section

4.1. GO Preparation

GO was made according to Hummer's method.[28] To be specific, 3.0 g graphite flakes were mixed with 1.5 g $NaNO_3$ then cooled to 0 °C. 69 mL H_2SO_4 (98 wt%, Sigma Aldrich) was added to the mixture and stirred uniformly before 9.0 g $KMnO_4$ was added slowly to the mixture. The reaction temperature was kept below 20 °C while adding the $KMnO_4$. After that, the reaction was warmed to 35 °C and stirred for 30 min. Then 138 mL distilled water was added slowly to the mixture while maintaining the reaction temperature at 98 °C for 15 min. The mixture was then cooled down and additional 420 mL water and 3 mL 30% H_2O_2 were added. After cooling in air, the mixture was washed with distilled water in a filter. A GO cake was obtained and an aqueous GO solution was obtained after 30 min sonication.

4.2. NFC Preparation

NFC was fabricated according to the literature.[58] 78 mg TEMPO, 514 mg sodium bromide (NaBr) and 5 g Kraft bleached softwood pulp were mixed together. Then 30 mL of 12% NaClO was added to the mixture slowly to initiate TEMPO oxidation of the cellulose under gentle agitation. During the oxidation process, the pH was maintained at 10.5 by adding 1 mol/L NaOH. The reaction ended after the NaClO was consumed. After a TEMPO treatment, the fibers were thoroughly washed with distilled water and disintegrated by one pass through a Microfluidizer M-110EH (Microfluidics Ind., USA) to obtain a NFC suspension.

4.3. Highly Conductive Fiber Fabrication

GO+NFC gel solution was extruded directly into ethanol to form a GO+NFC fibrous gel. The fibrous gel was then pulled out to dry in air after 1 min of immersion. A pre-stressing force by hand was applied at the ends of the fibers during drying to improve the alignment of fibers. Highly conductive fibers were obtained by a carbonization of the GO+NFC precursor fibers in a 95% Ar_2 and 5% H_2 gas atmosphere. The heating process performed at a temperature ramped from room temperature to 400 °C with a heating rate of 30 °C/h, then further increase to 1000 °C with a heating rate of 200 °C/h. After that, the samples are held for 2 h under 1000 °C. Conductive NFC microfibers and GO microfibers were fabricated with the same process. Ethanol with 1 wt% NaOH was chosen as the coagulation bath for GO fiber preparation. The reason is that GO dissolves in ethanol; thus with the coagulation bath of pure ethanol, no GO fibers can be obtained. Improving the alignment and packing density of building blocks can largely increase the fiber conductivity.[8] Good alignment and a high packing density results in a high strength for the precursor fibers. GO+NFC precursor fibers with GO:NFC weight ratios of 2:1, 1:1, and 1:2 were made. When the weight ratio of GO:NFC was 1:1, the fibers were stronger and were chosen as the precursor fiber to make conductive fiber. The conductivity of carbonized fiber was calculated from the *I–V* curve, which was plotted by measuring current at a given voltage. Silver paste was applied on the end of the fiber and used as a contact point. The fiber length and average diameter were measured by optical microscopy. When calculating the conductivity, the fiber was assumed to be perfect round shape, solid fiber.

4.4. Lithium Ion Battery Assembling and Testing

A half-cell with c(GO+NFC) fibers as the working electrode and lithium metal as the counter electrode was assembled into a coin cell for an electrochemical test. The separator and 2025 coin cell were purchased from MTI Inc. A solution of 1 M $LiPF_6$ in ethylene carbonate (EC)-diethyl carbonate (DEC) served as the electrolyte. The assembled cells were tested using a Biologic VMP3 electrochemical potentiostat in the potential range of 0.05–2.0 V at 25 mA/g.

Supporting Information

Supporting Information is available from the Wiley Online Library or from the author.

Acknowledgements

L. Hu acknowledges the support from the DOD (Air Force of Scientific Research) Young Investigator Program (FA95501310143) and the startup support from the University of Maryland, College Park. Y. Li would like to thank the support by the Priority Academic Program Development of Jiangsu Higher Education Institutions (PAPD), the Graduate Student

Innovation Program of the Jiangsu Province (CXLX12_0531) and the Nanjing Forestry University Innovation Fund Program. We thank Colin Preston for the grammar check of this paper.

Received: June 27, 2014
Revised: August 16, 2014
Published online: September 16, 2014

[1] J. Ren, W. Y. Bai, G. Z. Guan, Y. Zhang, H. S. Peng, *Adv. Mater.* **2013**, *25*, 5965.
[2] M. Lee, C. Y. Chen, S. Wang, S. N. Cha, Y. J. Park, J. M. Kim, L. J. Chou, Z. L. Wang, *Adv. Mater.* **2012**, *24*, 1759.
[3] J. A. Lee, M. K. Shin, S. H. Kim, H. U. Cho, G. M. Spinks, G. G. Wallace, M. D. Lima, X. Lepro, M. E. Kozlov, R. H. Baughman, S. J. Kim, *Nat. Commun.* **2013**, *4*, 1970.
[4] J. Ren, L. Li, C. Chen, X. L. Chen, Z. B. Cai, L. B. Qiu, Y. G. Wang, X. R. Zhu, H. S. Peng, *Adv. Mater.* **2013**, *25*, 1155.
[5] H. H. Cheng, J. Liu, Y. Zhao, C. G. Hu, Z. P. Zhang, N. Chen, L. Jiang, L. T. Qu, *Angew. Chem. Int. Ed.* **2013**, *52*, 10482.
[6] T. Chen, S. T. Wang, Z. B. Yang, Q. Y. Feng, X. M. Sun, L. Li, Z. S. Wang, H. S. Peng, *Angew. Chem. Int. Ed.* **2011**, *50*, 1815.
[7] W. Lu, M. Zu, J. Byun, B. Kim, T. Chou, *Adv. Mater.* **2012**, *24*, 1805.
[8] N. Behabtu, C. C. Young, D. E. Tsentalovich, O. Kleinerman, X. Wang, A. W. K. Ma, E. A. Bengio, R. F. ter Waarbeek, J. J. de Jong, R. E. Hoogerwerf, S. B. Fairchild, J. B. Ferguson, B. Maruyama, J. Kono, Y. Talmon, Y. Cohen, M. J. Otto, M. Pasquali, *Science* **2013**, *339*, 182.
[9] R. J. Sammons, J. R. Collier, T. G. Rials, J. E. Spruiell, S. Petrovan, *J. Appl. Polym. Sci.* **2013**, *128*, 951.
[10] N. H. Phan, S. Rio, C. Faur, L. Le Coq, P. Le Cloirec, T. H. Nguyen, *Carbon* **2006**, *44*, 2569.
[11] E. Frank, L. M. Steudle, D. Ingildeev, J. M. Spörl, M. R. Buchmeiser, *Angew. Chem. Int. Ed.* **2014**, *53*, 5262.
[12] X. W. Lu, P. J. Pellechia, J. R. V. Flora, N. D. Berge, *Bioresource Technol.* **2013**, *138*, 180.
[13] L. P. Wang, C. Schütz, S. A. German, M. M. Titirici, *RSC Adv.* **2014**, *4*, 17549.
[14] A. G. Dumanli, A. H. Windle, *J. Mater. Sci.* **2012**, *47*, 4236.
[15] M. Sevilla, A. B. Fuertes, *Carbon* **2009**, *47*, 2281.
[16] T. V. Cuong, V. H. Pham, T. T. Quang, J. S. Chung, E. W. Shin, J. S. Kim, E. J. Kim, *Mater. Lett.* **2010**, *64*, 765.
[17] Y. R. Rhim, D. J. Zhang, D. H. Fairbrother, K. A. Wepasnick, K. J. Livi, R. J. Bodnar, D. C. Nagle, *Carbon* **2010**, *48*, 1012.
[18] S. Stankovich, D. A. Dikin, G. H. B. Dommett, K. M. Kohlhaas, E. J. Zimney, E. A. Stach, R. D. Piner, S. T. Nguyen, R. S. Ruoff, *Nature* **2006**, *442*, 282.
[19] G. Zhao, J. Li, L. Jiang, H. Dong, X. Wang, W. Hu, *Chem. Sci.* **2012**, *3*, 433.
[20] T. Xie, W. Lv, W. Wei, Z. Li, B. Li, F. Kang, Q. H. Yang, *Chem. Commun.* **2013**, *49*, 10427.
[21] X. Xie, C. Zhang, M.-B. Wu, Y. Tao, W. Lv, Q.-H. Yang, *Chem. Commun.* **2013**, *49*, 11092.
[22] H. Zhu, C. Xiao, H. Cheng, F. Grote, X. Zhang, T. Yao, Z. Li, C. Wang, S. Wei, Y. Lei, Y. Xie, *Nat. Commun.* **2014**, *5*, 3960.
[23] D. Papkov, A. Moravsky, O. C. Compton, Z. An, X. Z. Li, S. T. Nguyen, Y. A. Dzenis, *Adv. Func. Mater.* **2013**, *23*, 5763.
[24] D. Krishnan, K. Raidongia, J. J. Shao, J. X. Huang, *ACS Nano.* **2014**, *8*, 449.
[25] G. J. Huang, C. Y. Hou, Y. L. Shao, H. Z. Wang, Q. H. Zhang, Y. G. Li, M. F. Zhu, *Sci. Rep.*, **2014**, *4*, 4248.
[26] R. C. Silva, A. M. Gomez, H. I. Kim, H. K. Jang, F. Tristan, S. V. Diaz, L. P. Rajukumar, A. L. Elías, N. P. Lopez, J. Suhr, M. Endo, M. Terrones, *ACS Nano* **2014**, *8*, 5959.
[27] X. W. Lu, J. R. V. Flora, N. D. Berge, *Bioresource Technol.* **2014**, *154*, 229.
[28] D. C. Marcano, D. V. Kosynkin, J. M. Berlin, A. Sinitskii, Z. Z. Sun, A. Slesarev, L. B. Alemany, W. Lu, J. M. Tour, *ACS Nano* **2010**, *4*, 4806.
[29] X. Z. Hu, Z. Xu, C. Gao, *Sci. Rep.* **2012**, *2*, 767.
[30] S. M. Kang, X. H. Li, J. Fan, J. Chang, *Ind. Eng. Chem. Res.* **2012**, *51*, 9023.
[31] R. Rozada, J. I. Paredes, S. Villar-Rodil, A. Martinez-Alonso, J. M. D. Tascon, *Nano Res.* **2013**, *6*, 216.
[32] B. Y. Dai, L. Fu, L. Liao, N. Liu, K. Yan, Y. S. Chen, Z. F. Liu, *Nano Res.* **2011**, *4*, 434.
[33] N. Behabtu, M. J. Green, M. Pasquali, *Nano Today* **2008**, *3*, 24.
[34] K. N. Kudin, B. Ozbas, H. C. Schniepp, R. K. Prud'homme, I. A. Aksay, R. Car, *Nano Lett.* **2008**, *8*, 36.
[35] V. Lopez, R. S. Sundaram, C. Gomez-Navarro, D. Olea, M. Burghard, J. Gomez-Herrero, F. Zamora, K. Kern, *Adv. Mater.* **2009**, *21*, 4683.
[36] H. P. Cong, X. C. Ren, P. Wang, S. H. Yu, *Sci. Rep.* **2012**, *2*, 613.
[37] Z. Xu, C. Gao, *Nat. Commun.* **2011**, *2*, 571.
[38] Z. Xu, Y. Zhang, P. G. Li, C. Gao, *ACS Nano.* **2012**, *6*, 7103.
[39] E. Y. Jang, J. Carretero-Gonzalez, A. Choi, W. J. Kim, M. E. Kozlov, T. Kim, T. J. Kang, S. J. Baek, D. W. Kim, Y. W. Park, R. H. Baughman, Y. H. Kim, *Nanotechnology* **2012**, *23*, 235601.
[40] Z. L. Dong, C. C. Jiang, H. H. Cheng, Y. Zhao, G. Q. Shi, L. Jiang, L. T. Qu, *Adv. Mater.* **2012**, *24*, 1856.
[41] Y. N. Meng, Y. Zhao, C. G. Hu, H. H. Cheng, Y. Hu, Z. P. Zhang, G. Q. Shi, L. T. Qu, *Adv. Mater.* **2013**, *25*, 2326.
[42] Z. Xu, H. Y. Sun, X. L. Zhao, C. Gao, *Adv. Mater.* **2013**, *25*, 188.
[43] C. S. Xiang, N. Behabtu, Y. D. Liu, H. G. Chae, C. C. Young, B. Genorio, D. E. Tsentalovich, C. G. Zhang, D. V. Kosynkin, J. R. Lomeda, C. C. Hwang, S. Kumar, M. Pasquali, J. M. Tour, *ACS Nano* **2013**, *7*, 1628.
[44] C. S. Xiang, C. C. Young, X. Wang, Z. Yan, C. C. Hwang, G. Cerioti, J. Lin, J. Kono, M. Pasquali, J. M. Tour, *Adv. Mater.* **2013**, *25*, 4592.
[45] L. Chen, Y. L. He, S. G. Chai, H. Qiang, F. Chen, Q. Fu, *Nanoscale* **2013**, *5*, 5809.
[46] X. M. Li, T. S. Zhao, K. L. Wang, Y. Yang, J. Q. Wei, F. Y. Kang, D. H. Wu, H. W. Zhu, *Langmuir* **2011**, *27*, 12164.
[47] X. L. Zhao, Z. Xu, B. N. Zheng, C. Gao, *Sci. Rep.* **2013**, *3*, 3164.
[48] C. G. Hu, Y. Zhao, H. H. Cheng, Y. H. Wang, Z. L. Dong, C. C. Jiang, X. Q. Zhai, L. Jiang, L. T. Qu, *Nano Lett.* **2012**, *12*, 5879.
[49] H. Sun, X. You, J. Deng, X. L. Chen, Z. B. Yang, J. Ren, H. S. Peng, *Adv. Mater.* **2014**, *26*, 2868.
[50] Z. B. Yang, H. Sun, T. Chen, L. B. Qiu, Y. F. Luo, H. S. Peng, *Angew. Chem. Int. Ed.* **2013**, *52*, 7545.
[51] Z. S. Tian, C. X. Xu, J. T. Li, G. Y. Zhu, Z. L. Shi, Y. Lin, *ACS Appl. Mater. Interf.* **2013**, *5*, 1489.
[52] S. H. Aboutalebi, R. Jalili, D. Esrafilzadeh, M. Salari, Z. Gholamvand, S. A. Yamini, K. Konstantinov, R. L. Shepherd, J. Chen, S. E. Moulton, P. C. Innis, A. I. Minett, J. M. Razal, G. G. Wallace, *ACS Nano* **2014**, *8*, 2456.
[53] X. Z. Hu, Z. Xu, Z. Liu, C. Gao, *Sci. Rep.* **2013**, *3*, 2374.
[54] H. C. Schniepp, J. L. Li, M. J. McAllister, H. Sai, M. Herrera-Alonso, D. H. Adamson, R. K. Prud'homme, R. Car, D. A. Saville, I. A. Aksay, *J. Phys. Chem. B*, **2006**, *110*, 8535.
[55] D. H. Cho, J. M. Kim, D. Y. Kim, *Mater. Lett.* **2013**, *104*, 24.
[56] J. P. de Mesquita, L. S. Reis, A. D. Purceno, C. L. Donnici, R. M. Lago, F. V. Pereira, *J. Chem. Techn. Biotech.* **2013**, *88*, 1130.
[57] L. B. Deng, R. J. Young, I. A. Kinloch, Y. Q. Zhu, S. J. Eichhorn, *Carbon* **2013**, *58*, 66.
[58] Y. Y. Li, H. L. Zhu, H. B. Gu, H. Q. Dai, Z. Q. Fang, N. J. Weadock, Z. H. Guo, L. B. Hu, *J. Mater. Chem. A* **2013**, *1*, 15278.